Combined X-ray diffraction and kinetic depth effect imaging

Anthony Dicken,[1,*] Keith Rogers,[1] Paul Evans,[2] Jer Wang Chan,[2] Joseph Rogers[1] and Simon Godber[2]

[1]*Cranfield Forensic Institute, Cranfield University, Shrivenham, Swindon, SN68LA, UK.*
[2]*The Imaging Science Group, School of Science and Technology, Nottingham Trent University, Nottingham, UK.*
**a.dicken@cranfield.ac.uk*

Abstract: In this preliminary study we present a depth resolved transmission image sequence of an object combined with the materials discriminating ability of angular dispersive X-ray diffraction. Volumes within the object giving rise to diffraction patterns matched to a library of specific materials have been encoded visually within the images. The intensity of these highlighted areas has been weighted based on the certainty of the match. Both the theory and experimental proof of principle have been demonstrated. Considerations pertaining to a "scaled up" version of this technique are also discussed.

OCIS codes: (110.7440) X-ray imaging; (050.1940) Diffraction; (100.2980) Image enhancement.

References and links

1. J. P. O. Evans, and H. W. Hon, "Dynamic stereoscopic X-ray imaging," NDT Int. **35**(5), 337–345 (2002).
2. S. Singh, and M. Singh, "Explosive detection systems (EDS) for aviation security," Signal Process. **83**(1), 31–55 (2003).
3. M. Marshall and J. Oxley, *Aspects of Explosives Detection* (Elsevier 2009).
4. J. P. O. Evans, Y. Liu, J. W. Chan, and D. Downes, "View synthesis for depth from motion 3D X-ray imaging," Pattern Recognit. Lett. **27**(15), 1863–1873 (2006).
5. K. W. Loschke, and W. L. Dunn, "Detection of chemical explosives using multiple photon signatures," Appl. Radiat. Isot. **68**(4-5), 884–887 (2010).
6. J. D. Lowrey, and W. L. Dunn, "Signature-based radiation scanning using radiation interrogation to detect explosives," Appl. Radiat. Isot. **68**(4-5), 893–895 (2010).
7. S. Singh, "Sensors--an effective approach for the detection of explosives," J. Hazard. Mater. **144**(1-2), 15–28 (2007).
8. C. Kottler, V. Revol, R. Kaufmann, and C. Urban, "Dual energy phase contrast x-ray imaging with Talbot-Lau interferometer," J. Appl. Phys. **108**(11), 114906 (2010).
9. M. J. Kitchen, D. M. Paganin, K. Uesugi, B. J. Allison, R. A. Lewis, S. B. Hooper, and K. M. Pavlov, "Phase contrast image segmentation using a Laue analyser crystal," Phys. Med. Biol. **56**(3), 515–534 (2011).
10. H. Vogel, "Search by X-rays applied technology," Eur. J. Radiol. **63**(2), 227–236 (2007).
11. G. Harding, "X-ray diffraction imaging--a multi-generational perspective," Appl. Radiat. Isot. **67**(2), 287–295 (2009).
12. B. Sun, M. Li, F. Zhang, Y. Zhong, N. Kang, W. Lu, and J. Liu, "The performance of a fast testing system for illicit materials detection based on energy-dispersive X-ray diffraction technique," Microchem. J. **95**(2), 293–297 (2010).
13. S. J. Wilkinson, K. D. Rogers, C. J. Hall, R. A. Lewis, A. Round, S. E. Pinder, C. Boggis, and A. Hufton, "Small angle diffraction imaging for disease diagnosis," Nucl. Instrum. Methods Phys. Res. A **548**(1-2), 135–139 (2005).
14. S. Pani, E. J. Cook, J. A. Horrocks, J. L. Jones, and R. D. Speller, "Characterization of breast tissue using energy-dispersive X-ray diffraction computed tomography," Appl. Radiat. Isot. **68**(10), 1980–1987 (2010).
15. B. C. Larson, W. Yang, G. E. Ice, J. D. Budai, and J. Z. Tischler, "Three-dimensional X-ray structural microscopy with submicrometre resolution," Nature **415**(6874), 887–890 (2002).
16. B. Jakobsen, H. F. Poulsen, U. Lienert, J. Almer, S. D. Shastri, H. O. Sørensen, C. Gundlach, and W. Pantleon, "Formation and subdivision of deformation structures during plastic deformation," Science **312**(5775), 889–892 (2006).
17. R. J. Cernik, K. H. Khor, and C. Hansson, "X-ray colour imaging," J. R. Soc. Interface **5**(21), 477–481 (2008).

#141311 - $15.00 USD Received 21 Jan 2011; revised 4 Mar 2011; accepted 7 Mar 2011; published 21 Mar 2011

18. G. Harding, "X-ray diffraction imaging--a multi-generational perspective," Appl. Radiat. Isot. **67**(2), 287–295 (2009).
19. C. H. Malden, and R. D. Speller, "A CdZnTe array for the detection of explosives in baggage by energy-dispersive X-ray diffraction signature at multiple scatter angles," Nucl. Instrum. Methods Phys. Res. A **449**(1-2), 408–415 (2000).
20. A. Dicken, K. Rogers, P. Evans, J. Rogers, and J. W. Chan, "The separation of X-ray diffraction patterns for threat detection," Appl. Radiat. Isot. **68**(3), 439–443 (2010).
21. A. Dicken, K. Rogers, P. Evans, J. Rogers, J. W. Chan, and X. Wang, "Position determination of scatter signatures--a novel sensor geometry," Talanta **83**(2), 431–435 (2010).
22. E. J. Cook, J. A. Griffiths, M. Koutalonis, C. Gent, S. Pani, J. A. Horrocks, L. George, S. Hardwick, and R. Speller, "Illicit drug detection using energy dispersive X-ray diffraction", Proc of SPIE **Vol 7310** (2009).
23. B. D. Cullity, *Elements of X-ray Diffraction* (Addison-Wesley Publishing Company Inc 1956).
24. K. Rogers, P. Evans, J. Rogers, J. W. Chan, and A. Dicken, "Focal construct geometry – a novel approach to the acquisition of diffraction data," J. Appl. Cryst. **43**(2), 264–268 (2010).

1. Introduction

The development of rapid 3 dimension imaging for the reconstruction of volumetric information has impacted within an increasing number of fields including materials science, medicine and security screening. However, the aim of such imaging is often to identify the distribution (or presence) of a specific material or range of materials within a volume and this is generally not available through current imaging modalities. For example, the screening of luggage to detect the presence of prohibited materials is a problem that still lacks a comprehensive solution.

Whereas absorption based image acquisition methods have developed into high resolution, volumetric visualisation tools such as stereoscopy [1, 2], computerized tomography (CT) [2, 3] and kinetic depth effect X-ray (KDEX) techniques [4], there has been little concomitant development of complementary chemical identification methodologies. The demand for such methods is well demonstrated, for example, with the need to identify explosives within luggage [5–7] that may have an innocuous shape. Qualitative materials discrimination is currently mostly limited to dual-energy imaging which has also been applied recently to very high spatial resolution phase contrast imaging [8, 9], although material's identification methods remains under development.

X-ray diffraction is a well established technique that is routinely used within laboratories for materials identification. It has been shown to be an effective probe for chemically identifying concealed explosives [10–12] and can identify biochemical changes accompanying the onset of cancer [13, 14]. The 'fingerprint' scattering signatures [12] produced from a diffraction experiment can thus be used as a highly specific marker of particular materials even within a mixture of several materials. High resolution, 3D chemico-structural probes have been developed to characterise microstructures for both static [15] and dynamic studies [16]. Perhaps the most advanced diffraction imaging system is 'TEDDI' [17] which provides tomographic diffraction imaging and has evolved to accommodate relatively high X-ray energies. The 'gold standard' for definitive materials analysis from diffraction employs monochromatic X-rays and an angularly dispersive data collection approach. In contrast, often when diffracted X-rays have been used previously to complement absorption imaging an energy dispersive approach has been adopted [14, 17, 18]. Here characteristic diffraction patterns are obtained from individual locations within an inspection volume that have been illuminated by white radiation. Restricting the directionality of the primary and scattering X-rays via collimation provides positional information at the expense of overall beam flux [19].

We have been pursuing alternative angular dispersive configurations [20, 21] (because of their inherently superior specificity [22]) that crucially do not require scattering collimation. The limitation of such chemically specific techniques applied in isolation is that not all prohibited materials are chemically distinct. Knives and scissors are not readily distinguished from innocuous metals based on their chemical structure. Therefore any chemical technique needs to complement conventional imaging technology rather than replace it.

#141311 - $15.00 USD Received 21 Jan 2011; revised 4 Mar 2011; accepted 7 Mar 2011; published 21 Mar 2011

Our study demonstrates the first X-ray image sequences of an inspection volume obtained via the imaging technique, KDEX that has simultaneously been interrogated by X-ray diffraction. Areas giving rise to diffraction patterns matched to a library of specific materials have been encoded visually within the images. Furthermore the intensity of these highlighted areas has been weighted based on the certainty of the match. It should be noted that this preliminary study has been conducted with molybdenum radiation (K alpha ≈17keV) which is somewhat lower energy than tungsten radiation (K alpha ≈59keV) traditionally employed for baggage and medical imaging. However, the benefits demonstrated by this work may one day translate to a scaled up system operating at higher energies. Some of the issues involved in a scale up have been addressed in section 4.

1.1 Principles of X-ray coherent scatter

The majority of materials are polycrystalline or semi-crystalline. For this reason a powder diffraction model has been adopted employing a kinematic approximation. If a mono-energetic X-ray beam strikes a material with long range order, then a proportion is absorbed and then remitted isotropically. Constructive and destructive interference effects result in radiation being scattered at characteristic angles [23]. These angles are directly related to interplanar spacing's (d) within the material and are governed by Braggs law. Once the d-spacings of a material have been determined these are matched against a reference library to provide an identification. An important consideration is the experimental geometry and, in particular, the relative positions of sample and detector. If the relationship between the incident beam direction, the sample position and the detector position is ill described then the correct angles of diffraction cannot be calculated.

1.2 Determining the spatial origin of scatter signatures

We have employed an open collimation system and thus Bragg maxima from any diffracting material illuminated by the primary pencil beam can subsequently strike the detector. However, for objects extended along the primary beam Bragg maxima from multiple unknown positions may contribute to the resulting diffraction pattern. Previous work [21] has examined a possible solution that uses an X-ray detector translated to a series of positions along the primary beam path (illustrated in Fig. 1b). A peak tracking algorithm is then applied that searches the patterns for Bragg maxima positions that linearly propagate through the detector positions. The gradient of these linearly propagating Bragg maxima positions provides the diffraction angle (2θ). Back projecting the linear propagation provides the origin within the inspection volume. As a result the sample to detector distance of any diffracting materials (sample position) and Bragg diffraction angle can be determined simultaneously. A more detailed description of this approach can be found in Dicken et al [21].

1.3 Principles of kinetic depth effect X-ray (KDEX)

KDEX provides the ability to visualise an inspection volume in 3D and is therefore comparable to CT. However CT scanners often require many projections to reconstruct a volumetric image [2, 4] and this is costly in time. KDEX operates similarly in that it requires multiple views to provide its 3D effect, however the number of images it requires is typically an order of magnitude lower and there is no reconstruction penalty. A parallax effect is brought about by differences in angular velocity of individual objects within an in inspection volume. Thus depth perception is afforded through this parallax [4]. Another important consideration is that the linear detector arrays used to produce the primary images can be arranged within an inspection tunnel in such a manner as they do not increase data acquisition time from that of a single detector system [4].

KDEX and X-ray diffraction then provide significantly different, complementary information concerning characteristics of any inspection volume. This work seeks, for the first

#141311 - $15.00 USD Received 21 Jan 2011; revised 4 Mar 2011; accepted 7 Mar 2011; published 21 Mar 2011

time, to combine these approaches and realise an unprecedented, materials specific imaging technique.

2. Method and materials

A 3D small scale phantom object was constructed that contained an alumina component (the 'target' material) as well as other scattering and attenuating objects overlapped in depth (illustrated in Fig. 2). X-rays were produced by a Philips PW1830 X-ray generator incorporating a sealed, long fine focus X-ray tube with a molybdenum target. A cooled (–40°C) PIXIS 1024 x 1024 16bit CCD camera with a Gd_2O_2S:Tb phosphorous screen was used to detect the X-rays. A selection of Thorlab and Sigma-koki translation stages were used to move various components namely the phantom and camera through multiple axes. To obtain the KDEX image sequences, multiple images were collected after the object was rotated through 1° increments from +15° to −15° of the rotation axis whilst the X-ray source and detector remained stationary (illustrated in Fig. 1a). This is equivalent to the traditional KDEX geometry where the object remains stationary and source and detector are rotated [4]. The X-ray diffraction patterns were collected by collimating the X-rays into a pencil beam with a 4 mm thick brass plate and 0.66 mm diameter aperture (illustrated in Fig. 1b). A set of translation stages were then used to systematically move the sample across the pencil beam. The PIXIS camera was used in raster scan mode to collect the diffraction patterns propagating normal to the primary beam path. This operation was repeated at differing distances along the primary beam path so that multiple diffraction patterns could be collected for each interrogated point on the sample. 28 points (equating to a 4 x 7 grid) on the sample were inspected. Four diffraction patterns were collected per point. It should be noted that all diffraction patterns were collected from the inspection volume when it was at 0°. Camera exposure times were quite different for the KDEX and diffraction aspects (4 seconds per image and 3 minutes per diffraction pattern respectively). This is because only a small proportion (<<1%) of the primary beam is coherently scattered. It should also be noted that although currently each aspect is collected consecutively, it is hoped that sophisticated collimation could enable both aspects to be obtained simultaneously in the future.

For each diffraction interrogation point the four diffraction patterns were used by the peak tracking algorithm to determine both 2θ and position for each source of diffracted X-rays. These were subsequently compared to a limited material diffraction library to identify the materials. The number of Bragg maxima matching those of a target material for a particular location in a depth plane was used as an index of match certainty.

Material matches were then mapped onto all of the perspective images within the KDEX sequence using the peak tracking algorithm and a simple trigonometric function. Relative distances within the image sequence were calibrated using an internal standard (ruler apparent in the top left hand corner of Figs. 5 and 6).

To colour encode those positions identified as containing a target material the 16 bit tiff files were split into RGB components and the pixel values in the red channel were then multiplied by a weighting factor based on the number of target Bragg maxima identified in that region. In doing so the intensity of red reflects the index of match.

#141311 - $15.00 USD Received 21 Jan 2011; revised 4 Mar 2011; accepted 7 Mar 2011; published 21 Mar 2011

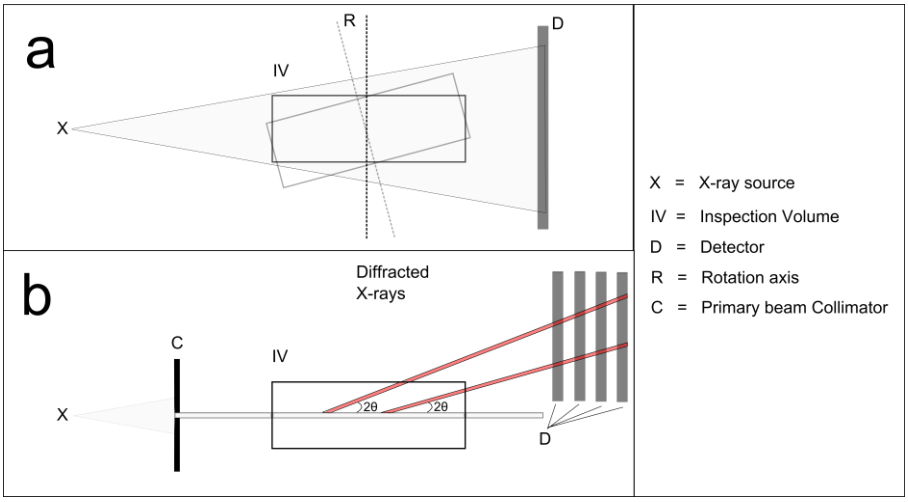

Fig. 1. A schematic illustrating the KDEX configuration (a) where the inspection volume is illustrated normal to the primary beam and a superposition at a given degree of rotation. The diffraction configuration (b) is also illustrated with the same detector positioned at differing distances along the primary beam path.

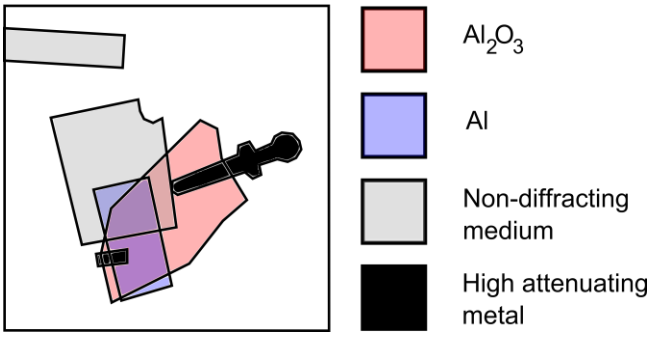

Fig. 2. Schematic illustrating the material composition of objects within the phantom.

3. Results

3.1 Peak finding algorithm

Examples of diffraction patterns measured at one interrogation point with different detector positions are shown in Fig. 3. The change in peak position between each detector location is a function of (i) the scattering angle and (ii) the diffraction source location along the primary beam. Figure 4 illustrates the positions (scattering angle) of a group of Bragg maxima tracked to a single location (±0.5 mm of each other) on the primary beam path within the inspection volume. These tracked Bragg maxima positions compare well with those for Al_2O_3 also demonstrated in Fig. 4 (the target in this example). Interrogation points that passed through other scattering materials (i.e Al) also gave rise to diffraction signatures but were tracked to a different location in the inspection volume. It should also be noted that although in this example only one material is targeted and identified the technique has been shown previously to resolve multiple unknown materials overlapped in depth [21].

#141311 - $15.00 USD Received 21 Jan 2011; revised 4 Mar 2011; accepted 7 Mar 2011; published 21 Mar 2011

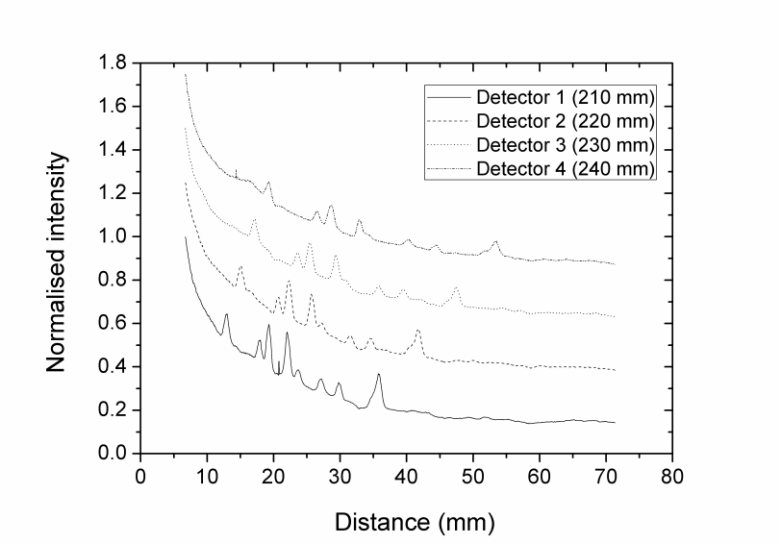

Fig. 3. Four diffraction patterns obtained from a single interrogated point in the inspection volume collected at specified distances along the primary beam path.

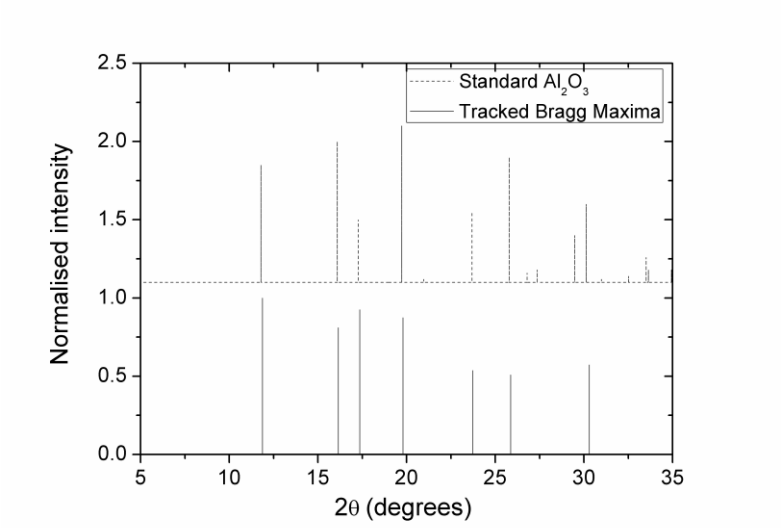

Fig. 4. Bragg maxima tracked to a single location in depth using the diffraction patterns illustrated in Fig. 3 and the peaking finding algorithm. The Bragg maxima correlate well with Al_2O_3.

3.2 Combined KDEX and diffraction imagery

The 0° KDEX image is illustrated in Fig. 5a and the diffraction inspection points are superimposed in Fig. 5b. Bragg maxima for each interrogated point were compared to a limited target database. Four points (indicated in Fig. 5c) were found to contain Bragg maxima consistent with the target material (Al_2O_3) at a specific depth within the object. It should be noted that these four points were the only ones to pass through the target material. The areas directly adjacent to the interrogated points with diffraction peaks corresponding to the target material were tagged. The red channel intensity values in these tagged areas were increased depending on the number of peaks that match the target diffraction pattern. Thus a greater red intensity indicates a greater confidence in the match between the unknown and

#141311 - $15.00 USD Received 21 Jan 2011; revised 4 Mar 2011; accepted 7 Mar 2011; published 21 Mar 2011

target material. Positions of the tagged areas were recalculated for the other KDEX perspectives using a trigonometric function and the position of the diffracting material produced by the peak tracking algorithm. This results in the tagged areas following the target material position within the transmission images. This effect is best appreciated when the images are demonstrated in a movie format. Figure 6 illustrates snapshots of the accompanying video at differing perspectives.

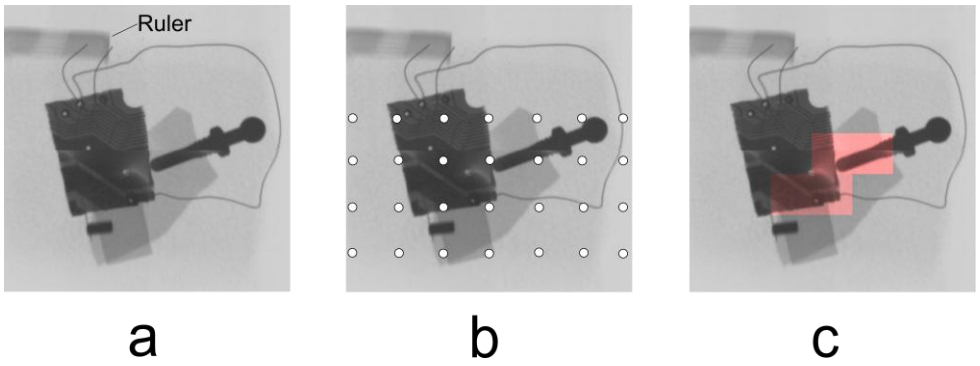

Fig. 5. A transmission image of the inspection volume at 0° rotation (a). The locations of the 28 interrogated positions that were illuminated by pencil beams (b). The tagged regions illustrating areas identified to contain threat materials (c). The end on projection of a ruler can be seen in the top left hand corner of each image, this can be better appreciated in the accompanying video.

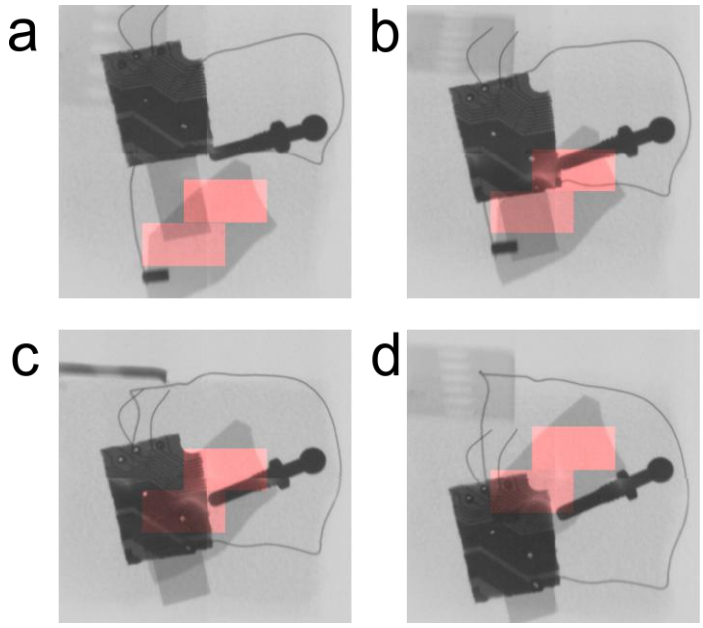

Fig. 6. Selected transmission images from a KDEX image sequence. Images are from –15° (a), –5° (b), +5° (c) and +15° (d) rotation of the inspection volume. Areas reported to have a target material based on their diffraction pattern have been colour encoded in red. The intensity of the red channel in the tagged areas reflects the certainty with which the area is believed to contain the target. (Media 1)

4. Discussion and conclusion

We have demonstrated that the 3-dimensional capability of the X-ray imaging technique, KDEX, has been combined with the material discriminating abilities of X-ray diffraction. The

#141311 - $15.00 USD Received 21 Jan 2011; revised 4 Mar 2011; accepted 7 Mar 2011; published 21 Mar 2011

fusion of these differing, complementary techniques has shown the potential to be a powerful diagnostic tool. The benefits of KDEX (i.e. the increase in morphological recognition performance in the presence of complicated structures) over conventional 2-dimensional (static) transmission imagery is realised with the simultaneous addition of chemically specific spatially resolved information. Potential applications are widespread (e.g. security screening). The radiographic identification of, for example, wiring within a bag, may be further and simultaneously investigated by chemcio-structural information provided by associated diffraction signatures which could indicate a threat.

This preliminary study has demonstrated great promise for a new diagnostic tool. However there are several issues that still need to be addressed. Coherently scattered X-rays are of several orders of magnitude lower in intensity than that of the principal X-ray beam. Efforts have been made here to increase the scattering flux by removing the need for scattering collimation. However data acquisition times probably require reducing further if the approach is to be exploited within real world applications. For such applications developments in detector and source technology must be made, although simple beam optics such as those demonstrated by Rogers et al [24] may provide a cost effective solution. Applications may also require a higher X-ray energy than that used here e.g. penetration in security screening applications requires typically >60keV. This energy "scale up" provides its own challenges, in particular a decrease in angular resolution. Moving the detectors further from the diffracting material should act as a positive optical lever (thus mitigating against the loss in angular resolution), however this is at the expense of the system sensitivity (also mentioned earlier) given the inverse squared law and additional air absorption. Presumably larger and/or more sensitive detectors would then be required. These technological improvements and modifications will need to be investigated for energy scale up, although niche markets involving the inspection of smaller attenuating volumes containing poly or semi-crystalline targets may find this technique valuable.

Acknowledgements

This ongoing programme of work is funded by EPSRC and is in collaboration with the UK Home Office Scientific Development Branch (HOSBD) and the US Department of Homeland Security (DHS).

#141311 - $15.00 USD Received 21 Jan 2011; revised 4 Mar 2011; accepted 7 Mar 2011; published 21 Mar 2011